Original Article

http://dx.doi.org/10.3348/kjr.2011.12.6.722
pISSN 1229-6929 · eISSN 2005-8330
Korean J Radiol 2011;12(6):722-730

Korean Journal of Radiology
KJR

Correlations of 3T DCE-MRI Quantitative Parameters with Microvessel Density in a Human-Colorectal-Cancer Xenograft Mouse Model

Sung Jun Ahn, MD[1], Chan Sik An, MD[1], Woong Sub Koom, MD[2], Ho-Taek Song, MD[1], Jin-Suck Suh, MD[1]

[1]Department of Radiology and Research Institute of Radiological Science, [2]Department of Radiation Oncology, College of Medicine, Yonsei University, Seoul 120-752, Korea

Objective: To investigate the correlation between quantitative dynamic contrast enhanced magnetic resonance imaging (DCE-MRI) parameters and microvascular density (MVD) in a human-colon-cancer xenograft mouse model using 3 Tesla MRI.

Materials and Methods: A human-colon-cancer xenograft model was produced by subcutaneously inoculating 1 x 10^6 DLD-1 human-colon-cancer cells into the right hind limbs of 10 mice. The tumors were allowed to grow for two weeks and then assessed using MRI. DCE-MRI was performed by tail vein injection of 0.3 mmol/kg of gadolinium. A region of interest (ROI) was drawn at the midpoints along the z-axes of the tumors, and a Tofts model analysis was performed. The quantitative parameters (K^{trans}, K_{ep} and V_e) from the whole transverse ROI and the hotspot ROI of the tumor were calculated. Immunohistochemical microvessel staining was performed and analyzed according to Weidner's criteria at the corresponding MRI sections. Additional Hematoxylin and Eosin staining was performed to evaluate tumor necrosis. The Mann-Whitney test and Spearman's rho correlation analysis were performed to prove the existence of a correlation between the quantitative parameters, necrosis, and MVD.

Results: Whole transverse ROI of the tumor showed no significant relationship between the MVD values and quantitative DCE-MRI parameters. In the hotspot ROI, there was a difference in MVD between low and high group of K^{trans} and K_{ep} that had marginally statistical significance (*ps* = 0.06 and 0.07, respectively). Also, K^{trans} and K_{ep} were found to have an inverse relationship with MVD (r = -0.61, p = 0.06 in K^{trans}; r = -0.60, p = 0.07 in K_{ep}).

Conclusion: Quantitative analysis of T1-weighted DCE-MRI using hotspot ROI may provide a better histologic match than whole transverse section ROI. Within the hotspots, K^{trans} and K_{ep} tend to have a reverse correlation with MVD in this colon cancer mouse model.

Index terms: *Colorectal cancer; MVD; Nude mouse model; Magnetic resonance imaging; Permeability; Angiogenesis; T1 dynamic contrast enhanced imaging; K^{trans}; DLD-1*

Received March 24, 2011; accepted after revision July 12, 2011.
This study was supported by a grant from the Korea Healthcare Technology R&D Project, Ministry of Health Welfare, Republic of Korea (A070001), and by the faculty research grant of Yonsei University College of Medicine (6-2008-0104), and by the KRIBB Research Initiative Program (KGS1211012). We would also like to acknowledge Siemens Healthcare Korea for technical support as part of a cooperative research and development agreement.
Corresponding author: Ho-Taek Song, MD, Department of Radiology, College of Medicine, Yonsei University, 50 Yonsei-ro, Seodaemun-gu, Seoul 120-752, Korea.
• Tel: (822) 2228-2370 • Fax: (822) 393-3035 • E-mail: hotsong@yuhs.ac

Korean Journal of Radiology
KJR

INTRODUCTION

Angiogenesis involves the formation of new capillaries from existing blood vessels and is an essential component of normal physiological as well as pathological processes. Tumors require angiogenesis for growth and tumor progression (1, 2). Methods for assessing the status of angiogenesis are valuable when evaluating cancer response to therapy. Microvessel density (MVD) has been used to evaluate the angiogenic activity of tumors (3). However, it does not reflect the functional status of the tumor vasculature, and invasive methods are necessary for obtaining specimens.

Permeability of a tumor vessel also reflects the angiogenic activity of the tumor (4, 5). T1 weighted dynamic contrast enhanced magnetic resonance imaging (DCE-MRI) has been proposed as a non-invasive method of assessing the permeability of the tumor vessel (6-9). Transendothelial permeability, capillary surface area, and lesion leakage space can be measured using quantitative parameters based on the two-compartment Tofts model on the condition that the exchange of contrast agent occurs only between the intravascular space and the tumor interstitial space (6). K^{trans} stands for the volume transfer constant of the contrast agent, determining the rate at which the contrast media passes from the intravascular space into the tumor interstitial space. The back diffusion of contrast agent from the interstitial space of the tumor into the intravascular space is determined by the rate constant K_{ep}. V_e represents the extravascular-extracellular leakage space. Because of the variability of derived quantitative parameters from T1-weighted DCE-MRI according to tissue characteristics and cancer type (7-9), correlating quantitative parameters with MVD would help to interpret the validity and meaning of the measured parameters. Reduction of microvessel blood flow after radiation therapy in locally advanced rectal cancer patients was correlated with decreased endothelial transfer coefficient value and MVD, as reported by de Lussanet et al. (10). Tuncbilek et al. (11) reported that the parameters from the time-intensity curves of DCE-MRI was correlated with postoperative MVD, histologic grade, and presence of metastasis. Zhang et al. (12) reported that the time to peak was negatively correlated with MVD and vascular endothelial growth factor (VEFG) in rectal cancer. Ceelen et al. (13) reported that radiation therapy reduces tumor vascular leakage and enhances tissue oxygenation, which was correlated with reduced K^{trans} and V_e of DEC-MRI and not correlated with MVD or VEGF expression in the colorectal tumor rat model.

In this study, we investigated the correlation between the quantitative DCE-MRI parameters and MVD in human-colon-cancer xenograft mouse models of various sizes using a clinical 3 Tesla (T) scanner.

MATERIALS AND METHODS

Experimental Model

The study protocol was approved by the local ethics committee for animal care and use. Experiments were performed in 10 adult (5-week-old) (SLC, Kotoh-cho, Japan) female nude mice, each weighing 17-20g. A human DLD-1 colon cancer cell suspension (1×10^6 cells in 100 μL phosphate buffered saline) was injected subcutaneously into the right hind limbs of the mice. Tumors were allowed to grow for approximately 7 to 14 days, until reaching a predetermined size, the longest diameter of which ranged from 0.6 cm to 2 cm.

Dynamic Contrast Enhanced MRI

All MRI studies were performed using a 3T MR scanner (MAGNETOM Tim Trio, Siemens Healthcare, Erlangen, Germany) with a four-phased array wrist coil. Mice were placed prone in a plastic holder for ease of fixation and injection of contrast agent, and an inhaled anesthesia was used to avoid movement during imaging. Anesthesia was maintained with 2% isoflurane in a mixture of 100% 1 L/min oxygen. The tail vein was cannulated for intravenous injection of gadolinium contrast agent.

All images were obtained in the transverse plane using the following sequences: transverse T2-weighted turbo spin-echo (TSE) sequence (repetition time [TR] msec/echo time [TE] msec) 4930/128, echo train length of 25, one signal acquired, matrix of 114 x 192) applied with a section thickness of 1.0 mm, an intersection gap of 1.1 mm, and a flip angle of 160°. The field of view was 35 x 60 mm^2, which included the tumor in its entirety (20 sections) with a resultant voxel size of 0.3 x 0.3 x 1.0 mm^3.

Dynamic contrast-enhanced MR imaging included two precontrast T1-weighted measurements (3D VIBE, TR/TE 8.3/2.3, 20 axial slices [slice thickness, 1.04 mm], field of view 50 x 50 mm, matrix 90 x 128) with different flip angles (2°, 15°) to determine the T1 relaxation time in the blood and tissue before the arrival of contrast agent on a pixel-by-pixel basis. This was followed by T1-measured

dynamic contrast-enhanced series using a TWIST sequence (TR/TE 5.8/2.4, flip angle of 12°, and all other parameters the same as for the precontrast image).

Sixty dynamic measurements were performed on the entire volume of 20 sections. The acquisition time was 6.2 seconds with a single dynamic measurement. After the first five measurements, an intravenous bolus of gadopentetate dimeglumine (Magnevist; Schering, Erlangen, Germany) at a concentration of 0.05 mmol/mL was administered by manual injection at a dose of 0.3 mmol/kg over a maximum period of five seconds. The results of a previous pilot study showed that this dose of contrast agent provides maximal signal enhancement with the same sequence used in this study (data not shown).

The scanned data were transferred onto an image processing workstation (Leonardo, Siemens Healthcare, Erlangen, Germany) and analyzed using Tissue4D® software (Siemens Healthcare, Erlangen, Germany). A value for the arterial input function was automatically calculated by the software without an arterial region of interest (ROI) measurement procedure. To verify the applicability of the programmed arterial input function, the enhancement pattern of the normal thigh muscles opposite to the tumor was also analyzed. All mice showed similar patterns of enhancement in muscle ROI, with minimal variation between animals.

Tumor ROI was drawn at the midpoint along the z-axis of the mass by a third-year resident under the supervision of a senior radiologist. Two ROIs were drawn and measured for each mouse. ROI 1 covered the whole transection area of the tumor. ROI 2 covered only the hotspot area in the tumor. Hotspots in the MR images were selected to be matched with a hotspot in immunohistochemical staining. Dynamic data from ROIs 1 and 2 were fitted pixel by pixel to a pharmacokinetic model described by Tofts et al. (6), of which the quantitative parameters K^{trans}, K_{ep}, and V_e, were calculated.

Histopathological Analysis

After DCE-MRI is performed, the tumor was dissected from the surrounding tissue under ether anesthesia and sterile conditions. The mice were euthanized at the end of the surgical procedure in a CO_2 chamber. The dissected tumor was fixed with 10% formaldehyde solution and preserved at 4°C for 24 hours. Then, 6 μm thick slide sections were made to correspond with the MR images. Immunohistochemical staining was also performed as follows: Deparaffinized slide sections were incubated with an anti-CD31 primary monoclonal antibody (Abcam, Cambridge, MA) followed by incubation with a biotinylated secondary antibody. The sections were then incubated with avidin-biotinylated peroxidase complex reagent and binding reactions were visualized using 3,3-diaminobenzidine (DAB). The stained microvessels were heterogeneous and the areas of highest neovascularization were mostly found at the periphery of the tumor. When scanned in a low-power field (100 x), highly vascularized areas were considered to be hotspots. Three hotspots were examined respectively and vessels were manually counted in a high-power field (200 x) with ocular grids. The grading and counting method described by Weidner et al. (14) was adapted for evaluation of MVD. Any brown-stained endothelial cell or endothelial cell cluster that was clearly separate from the adjacent microvessels, tumor cells, and other connective tissue elements was considered as a single countable microvessel. The sum of counts per field (total area = 0.578 mm^2) represented a single hotspot. The highest vessel count among the three hotspots was used as the MVD. Hematoxylin and Eosin staining was performed in a consecutive slide to confirm to tumor necrosis. The area including the hot spots was scanned with low-power fields (2 x, 40 x). The outer tumor border and tumor necrosis was manually circumscribed by using Image J software (NIH, Bethesda, MD). Then, the total pixel area of the tumor and necrotic region was automatically calculated. Histological necrotic fraction (NF) was defined as the division of total pixel area of necrosis by the total pixel area within the tumor border.

Statistical Analysis

The mice were divided into two subgroups according to their K^{trans}, K_{ep}, and V_e values. If a parameter was less than the median value, the mouse was assigned to the "low" group. And, if a parameter was above the median value, then the mouse was assigned to the "high" group. The Mann-Whitney test was performed to validate the differences in MVD between the low and high groups according to each parameter. The relationship between MVD, perfusion parameters and necrotic fraction of the tumor was examined by Spearman's correlation analysis. The correlation coefficient (τ) expresses the degree of change in the two corresponding variables. A coefficient closer to 1 indicates a positive correlation and a coefficient closer to -1 indicates a negative correlation. Statistical significance was accepted with a p value of less than 0.05. Statistical

Korean Journal of Radiology
KJR

analyses were performed using computer software (PASW Statistics 18; SPSS Inc., Chicago, IL).

RESULTS

Tumor size, DCE-MRI derived parameters, and MVD of 10 nude mice are summarized in Table 1. The range in tumor

Table 1. Summary of Quantitative T1-Weighted Dynamic Contrast Enhanced MRI Parameters, Size and Microvascular Density

No. (#)	Size (mm)	Whole Transverse Section (ROI 1)			Hotspots (ROI 2)			MVD (1/0.578 mm^2)	NF
		K^{trans} (Sec^{-1})	K_{ep} (Sec^{-1})	V_e	K^{trans} (Sec^{-1})	K_{ep} (Sec^{-1})	V_e		
1	6.9	0.118	3.054	0.091	0.173	3.631	0.085	71	0.29
2	7.4	0.285	6.341	0.063	0.429	9.675	0.05	53	0.03
3	8.1	0.098	2.105	0.12	0.301	8.039	0.041	59	0.22
4	9.2	0.112	2.727	0.078	0.301	6.486	0.077	58	0.14
5	10	0.141	3.552	0.079	0.299	6.32	0.061	64	0.36
6	10.2	0.168	3.739	0.051	0.269	5.624	0.065	69	0.02
7	12.1	0.188	4.463	0.07	0.293	6.864	0.044	69	0.11
8	12.7	0.147	3.412	0.09	0.278	6.133	0.083	119	0.05
9	16.1	0.072	3.398	0.072	0.334	6.888	0.093	78	0.04
10	16.4	0.113	3.042	0.054	0.237	5.393	0.053	108	0.31

Note.— MVD = microvascular density, NF = necrotic fraction: total pixel areas included in necrotic regions/total pixel areas included within tumor border

Table 2. Difference in Microvascular Density between Low and High Groups of Each Dynamic Contrast Enhanced MRI Parameter

	Whole Transverse Section (ROI 1)			Hotspots (ROI 2)		
	MVD		*P* Value	MVD		*P* Value
	Low	High		Low	High	
K^{trans}	71	69	0.84	71	59	0.06
K_{ep}	71	69	0.84	89.5	61.5	0.07
V_e	69	64	0.84	64	71	0.22

Note.— MVD = microvascular density, Low = group of mice with dynamic contrast enhanced MRI parameter values below median value, High = group of mice with dynamic contrast enhanced MRI parameter values above median value, MVD values are median. *P* value < 0.05 is considered to be statistically significant.

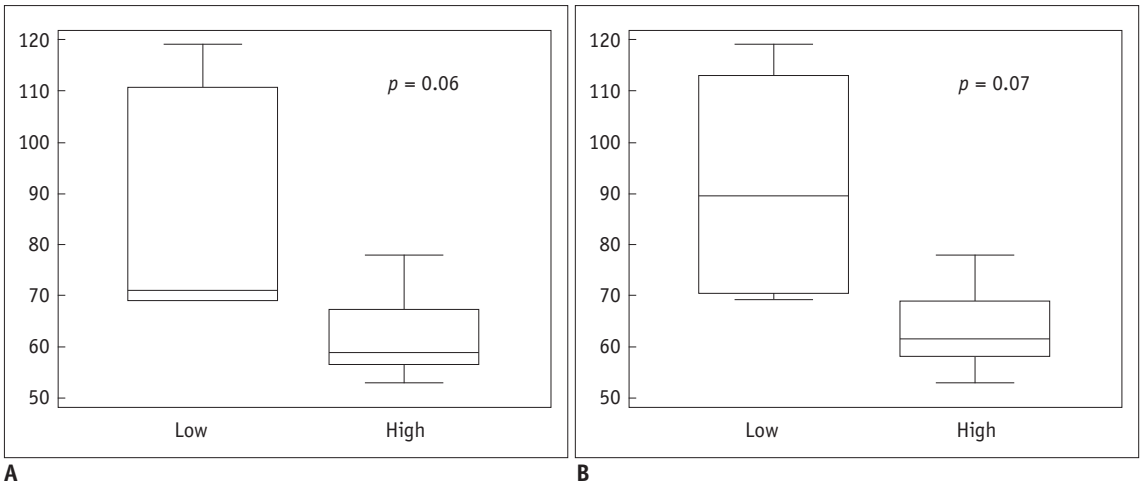

Fig. 1. Box whisker plot of microvascular density evaluating region of interest drawn on hotspots.
Distribution of low and high groups is shown in K^{trans} **(A)** and K_{ep} **(B)**.

size was 7.4 to 16.4 mm (average, 10.9 ± 3.3 mm). Table 2 describes the difference in the MVD value between the low and high value groups at each DCE-MRI parameter. In the case of the whole transverse ROI, there was no difference in MVD values between the low and high groups. However, in the case of hotspots, the median value of K^{trans} and K_{ep} in the low group was higher than that of the high group. Although these differences did not reach statistical significance (p = 0.06 in K^{trans}, p = 0.07 in K_{ep}), a box and whisker plot clearly showed the separated distribution of MVD of the two groups

Table 3. Relationship between Perfusion Parameters, Microvascular Density, and Tumor Necrotic Fraction

ROI 1	MVD		NF		ROI 2	MVD		NF	
	τ	*p*	τ	*p*		τ	*p*	τ	*p*
K^{trans}	-0.170	0.61	-0.370	0.27	K^{trans}	-0.610	0.06*	-0.340	0.31
K_{ep}	-0.109	0.74	-0.515	0.12	K_{ep}	-0.602	0.07*	-0.358	0.28
V_e	-0.012	0.97	0.455	0.17	V_e	0.492	0.14	-0.139	0.68

Note.— Correlation coefficient (τ) represents degree of change in two corresponding variables. *P* value < 0.05 is considered to be statistically significant. *Represents borderline statistical significance. MVD = microvascular density, NF = necrotic fraction, ROI 1 = whole transverse section, ROI 2 = hotspots

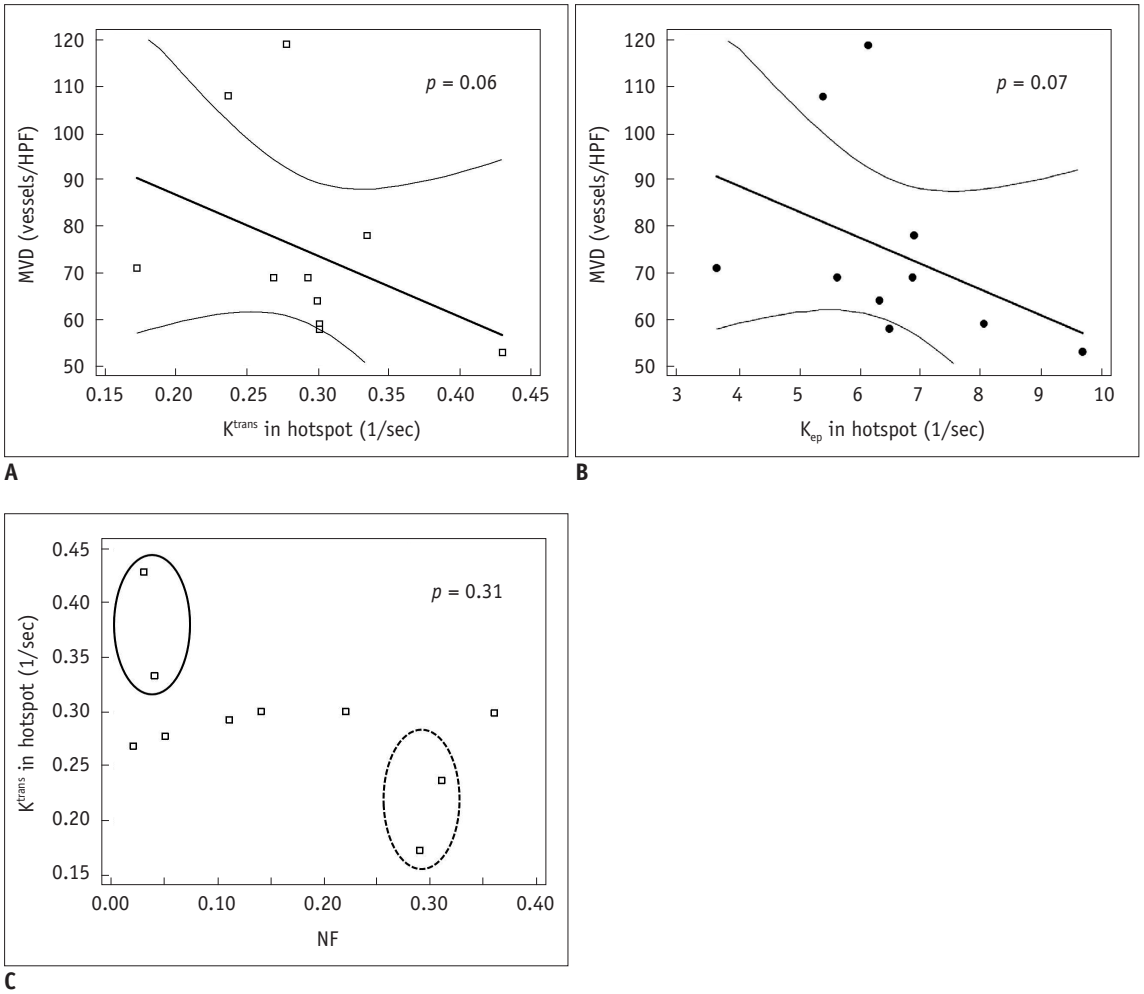

Fig. 2. Representative scatter diagrams showing relationships between microvascular density, necrotic fraction, and dynamic contrast enhanced MRI derived parameters from hotspots.
A, B. K^{trans} and microvascular density (Spearman's correlation = -0.61, p = 0.06) **(A)**, K_{ep} and microvascular density (Spearman's correlation = -0.60, p = 0.07) **(B)**. Dashed line indicates 95% confidence interval. **C.** Necrotic fraction and K^{trans} (Spearman's correlation = -0.34, p = 0.31). Solid circle represents group that shows low necrotic fraction and high K^{trans}. Dashed circle represents group who showed high necrotic fraction and low K^{trans}. MVD = microvascular density, NF = necrotic fraction

Korean Journal of Radiology
KJR

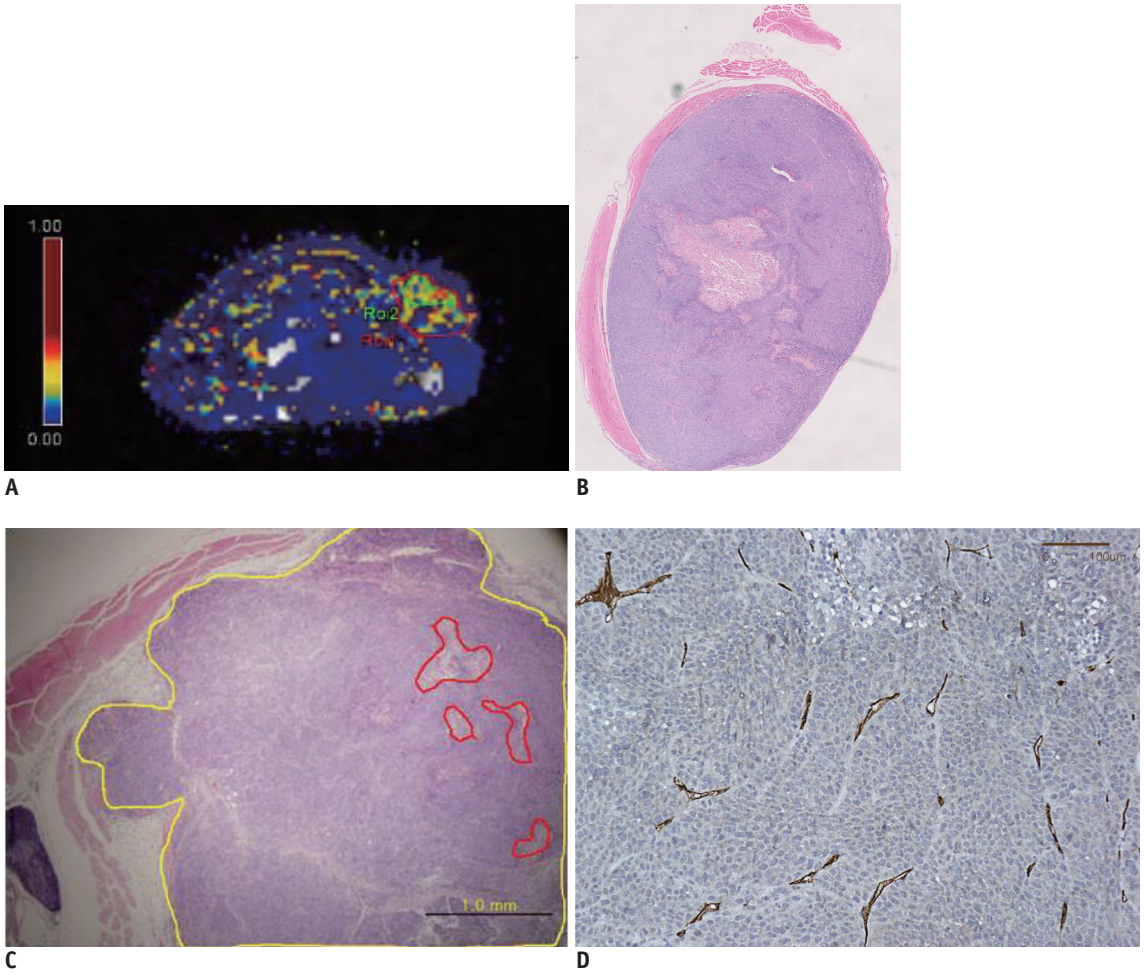

Fig. 3. Pixel-by-pixel analysis of K^{trans} in tumor of representative mouse #2 evaluated by dynamic contrast enhanced MRI with Tofts model.

A. K^{trans} values of whole tumor (ROI 1) and hotspot (ROI 2) are 0.285/sec and 0.429/sec, respectively. ROI 1 and ROI 2 are marked by red and green solid lines. **B.** Hematoxylin and Eosin staining of corresponding section of mouse #2 (original magnification, x 2). Necrosis is noted in center of tumor. **C.** Hematoxylin and Eosin staining includes hotspot area. Tumor necrosis fraction is 0.03 (original magnification, x 40). Yellow line indicates tumor border and red line indicates area of necrosis. **D.** CD 31 staining of tumor from mouse #2. Microvascular density count is 53 (original magnification, x 200).

(Fig. 1). According to Spearman's correlation analysis, perfusion parameters from whole transverse ROI did not show a significant relationship with MVD, while K^{trans} and K_{ep} from hotspot ROI showed marginally significant correlations with MVD (Table 3). Scatter diagrams demonstrated the inverse correlation between MVD with K^{trans} and K_{ep} (r = -0.61, p = 0.06 in K^{trans}; r = -0.60, p = 0.07 in K_{ep}) (Fig. 2). The necrotic fraction of the tumor did not show a significant relationship with the perfusion parameters regardless of ROI (p = 0.27 for K^{trans}, p = 0.12 for K_{ep}, p = 0.17 for V_e in whole transverse section and p = 0.37 for K^{trans}, p = 0.28 for K_{ep}, p = 0.68 for V_e in hotspots).

Images of the pixel-by-pixel K^{trans} analysis of the tumor and corresponding immunohistochemical staining of two representative mice are shown in Figure 3 and 4. The tumor in mouse #2 was one of the smallest with the largest diameter being 7.4 mm. Necrosis in the tumor was seldom found by histological staining. The K^{trans} and K_{ep} values were highest among the animals measured in the whole transverse ROI and also in the hotspot ROI, but their MVD values counted the lowest. The tumor from mouse #10 was the largest one with the largest diameter being 16.4 mm. The tumor showed massive necrosis at the center and cellularity was only preserved in the periphery. The K^{trans} and K_{ep} values were lower than in mouse #2 but the MVD value was 2nd highest among the animals.

DISCUSSION

T1-weighted DCE-MRI may be analyzed semi-

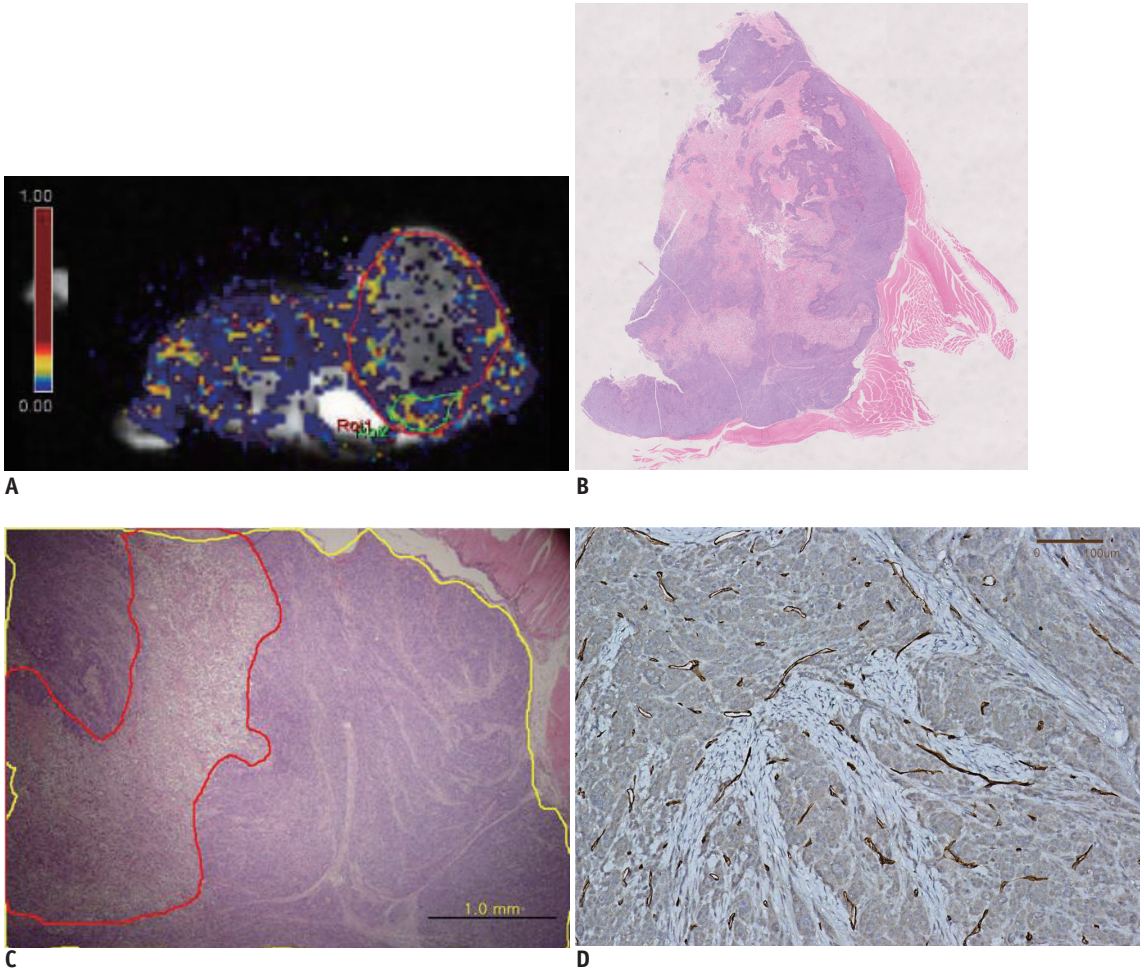

Fig. 4. Pixel by pixel analysis of K^{trans} in tumor of another representative mouse (#10).
A. K^{trans} values of whole tumors and hotspots were 0.113/sec and 0.237/sec respectively. ROI 1 and ROI 2 are marked by red and green solid lines, respectively. **B.** Hematoxylin and Eosin staining of corresponding section of mouse #10. Large amount of necrosis is shown (original magnification, x 2). **C.** Hematoxylin and Eosin staining including hotspot region. Tumor necrotic fraction is 0.31 (original magnification, x 40). Yellow line indicates tumor border and red line indicates area of necrosis. **D.** CD 31 staining of tissue from mouse #10. Microvascular density count is 108 (original magnification, x 200).

quantitatively (15) or quantitatively (6). For the semi-quantitative method, the slope of the time-intensity curve and the amplitude of the signal intensity are calculated directly from the curve. The semi-quantitative method could be influenced by scanner settings and might make inter-patient and inter-system comparisons difficult. Therefore, a quantitative analysis has been emphasized and it is necessary to explore the meaning of these parameters. Previous studies evaluated the relationship between semiquantitative values and MVD but there remained some controversy regarding the usefulness of semiquantitative DCE-MRI parameters in evaluating the angiogenic activity of the tumor (8, 11, 12, 16, 17). Studies using quantitative DCE-MRI parameters are also still in progress (10, 13, 18).

In this study, quantitative parameters were evaluated using the whole transverse section of the tumor slice (ROI 1) and the hotspot (ROI 2) to validate the effects of ROI selection and to minimize the effects of the necrotic area. This rapidly proliferating xenograft tumor model underwent necrosis in the central area. It would be reasonable to measure hotspots instead of whole tumor region when evaluating the status of the tumor using DCE-MRI parameters, since no correlation was proven between MVD and DCE MR parameters by using whole transverse ROI. Averaging the wide necrotic area in the tumor area negatively affected the evaluation of DCE-MRI parameters, regardless of the functional status of the tumor. A recent study by Galban et al. (19) stating that the parametric response map using the voxel-by-voxel registered comparison instead of the averaged ROI comparison in follow-up studies of brain tumor patients is a reliable imaging biomarker for early cancer treatment, and

Korean Journal of Radiology
KJR

the outcome also supports this study's results. Similarly, Stomper et al. (17) reported that the maximally enhanced area showed a broad correlation with MVD.

Although the inverse correlation of K^{trans} and K_{ep} with MVD was not statistically significant, likely due to the small sample size, it demonstrated that the feasibility that these parameters can be used to evaluate the angiogenic status of rapidly proliferating colon cancer. Lastly, K^{trans} or K_{ep} with MVD showed an inverse relationship. Generally, prior studies have supported a positive correlation between tissue perfusion and MVD (18). Sahani et al. (20) reported that the perfusion parameters in the high-grade hepatocellular carcinoma group were lower than the well-differentiated tumor group which was contrary to conventional belief; this observation was attributed to the presence of tumor necrosis. In the current study, tumors with large areas of necrosis (NF of 0.36 in mouse #5; NF of 0.31 in mouse #10) showed lower K^{trans} (0.299/sec, 0.237/sec respectively), while the tumors with small amounts of necrosis (NF of 0.03 in mouse #2; NF of 0.04 in mouse #9) showed higher K^{trans} (0.429/sec, 0.334/sec respectively). A scatter diagram (Fig. 2C) depicted the comparison of the two groups. Although the relationship between NF and perfusion parameter was not statistically significant ($p > 0.05$), this observation led to a reasoning that the degree of tumor necrosis may have affected the results. In addition, because MVD could not assess the functional status of the capillary wall, a high vessel count does not necessarily indicate high tissue perfusion.

Several shortcomings of our study should be noted. First, it was difficult to spatially co-localize histology with MR images. As a discrepancy was present between slice thickness in MRI versus a histological slide section (1.04 mm and 6 μm, respectively), a spatial mismatch was unavoidable. Also, tumor necrosis was not excluded in the whole transverse section (ROI 1). Thus, the quantitative parameter from the whole transverse section might not reflect the real tumor burden. And the meaning of the inverse correlation should be further investigated. Lastly, because quantitative parameters showed differences according to post-processing methods (21), our results should be carefully applied.

In conclusion, quantitative analysis of T1-weighted DCE-MRI using hotspot ROI may provide a better histologic match than using whole transverse section ROI. Within the hotspots, K^{trans} and K_{ep} tended to have a reverse correlation with MVD in this colon cancer mouse model.

REFERENCES

1. Folkman J. New perspectives in clinical oncology from angiogenesis research. *Eur J Cancer* 1996;32A:2534-2539
2. Rak JW, St Croix BD, Kerbel RS. Consequences of angiogenesis for tumor progression, metastasis and cancer therapy. *Anticancer Drugs* 1995;6:3-18
3. Vermeulen PB, Gasparini G, Fox SB, Toi M, Martin L, McCulloch P, et al. Quantification of angiogenesis in solid human tumours: an international consensus on the methodology and criteria of evaluation. *Eur J Cancer* 1996;32A:2474-2484
4. Deen S, Ball RY. Basement membrane and extracellular interstitial matrix components in bladder neoplasia--evidence of angiogenesis. *Histopathology* 1994;25:475-481
5. Nagy JA, Brown LF, Senger DR, Lanir N, Van de Water L, Dvorak AM, et al. Pathogenesis of tumor stroma generation: a critical role for leaky blood vessels and fibrin deposition. *Biochim Biophys Acta* 1989;948:305-326
6. Tofts PS, Brix G, Buckley DL, Evelhoch JL, Henderson E, Knopp MV, et al. Estimating kinetic parameters from dynamic contrast-enhanced T(1)-weighted MRI of a diffusable tracer: standardized quantities and symbols. *J Magn Reson Imaging* 1999;10:223-232
7. Hawighorst H, Knapstein PG, Weikel W, Knopp MV, Zuna I, Knof A, et al. Angiogenesis of uterine cervical carcinoma: characterization by pharmacokinetic magnetic resonance parameters and histological microvessel density with correlation to lymphatic involvement. *Cancer Res* 1997;57:4777-4786
8. Hulka CA, Edmister WB, Smith BL, Tan L, Sgroi DC, Campbell T, et al. Dynamic echo-planar imaging of the breast: experience in diagnosing breast carcinoma and correlation with tumor angiogenesis. *Radiology* 1997;205:837-842
9. Collins DJ, Padhani AR. Dynamic magnetic resonance imaging of tumor perfusion. Approaches and biomedical challenges. *IEEE Eng Med Biol Mag* 2004;23:65-83
10. de Lussanet QG, Backes WH, Griffioen AW, Padhani AR, Baeten CI, van Baardwijk A, et al. Dynamic contrast-enhanced magnetic resonance imaging of radiation therapy-induced microcirculation changes in rectal cancer. *Int J Radiat Oncol Biol Phys* 2005;63:1309-1315
11. Tuncbilek N, Karakas HM, Altaner S. Dynamic MRI in indirect estimation of microvessel density, histologic grade, and prognosis in colorectal adenocarcinomas. *Abdom Imaging* 2004;29:166-172
12. Zhang XM, Yu D, Zhang HL, Dai Y, Bi D, Liu Z, et al. 3D dynamic contrast-enhanced MRI of rectal carcinoma at 3T: correlation with microvascular density and vascular endothelial growth factor markers of tumor angiogenesis. *J Magn Reson Imaging* 2008;27:1309-1316
13. Ceelen W, Smeets P, Backes W, Van Damme N, Boterberg T, Demetter P, et al. Noninvasive monitoring of radiotherapy-induced microvascular changes using dynamic contrast enhanced magnetic resonance imaging (DCE-MRI) in

a colorectal tumor model. *Int J Radiat Oncol Biol Phys* 2006;64:1188-1196
14. Weidner N, Semple JP, Welch WR, Folkman J. Tumor angiogenesis and metastasis--correlation in invasive breast carcinoma. *N Engl J Med* 1991;324:1-8
15. Buadu LD, Murakami J, Murayama S, Hashiguchi N, Sakai S, Masuda K, et al. Breast lesions: correlation of contrast medium enhancement patterns on MR images with histopathologic findings and tumor angiogenesis. *Radiology* 1996;200:639-649
16. Cooper RA, Carrington BM, Loncaster JA, Todd SM, Davidson SE, Logue JP, et al. Tumour oxygenation levels correlate with dynamic contrast-enhanced magnetic resonance imaging parameters in carcinoma of the cervix. *Radiother Oncol* 2000;57:53-59
17. Stomper PC, Winston JS, Herman S, Klippenstein DL, Arredondo MA, Blumenson LE. Angiogenesis and dynamic MR imaging gadolinium enhancement of malignant and benign breast lesions. *Breast Cancer Res Treat* 1997;45:39-46
18. Schlemmer HP, Merkle J, Grobholz R, Jaeger T, Michel MS, Werner A, et al. Can pre-operative contrast-enhanced dynamic MR imaging for prostate cancer predict microvessel density in prostatectomy specimens? *Eur Radiol* 2004;14:309-317
19. Galban CJ, Chenevert TL, Meyer CR, Tsien C, Lawrence TS, Hamstra DA, et al. The parametric response map is an imaging biomarker for early cancer treatment outcome. *Nat Med* 2009;15:572-576
20. Sahani DV, Holalkere NS, Mueller PR, Zhu AX. Advanced hepatocellular carcinoma: CT perfusion of liver and tumor tissue--initial experience. *Radiology* 2007;243:736-743
21. Choi S, Liu H, Shin TB, Lee JH, Yoon SK, Oh JY, et al. Perfusion imaging of the brain using Z-score and dynamic images obtained by subtracting images from before and after contrast injection. *Korean J Radiol* 2004;5:143-148